Dynamic tune measurement methods during slow extraction

Claudia Carollo

claudiacarollo20@gmail.com

Summer Student Programme

September 2023

Supervisors:

E. Benedetto
R. Taylor
M. Vretenar

1 Introduction

The aim of NIMMS (Next Ion Medical Machine Study) at CERN is the development of technologies for the next generation of accelerators for ion therapy of cancer. In particular, the focus is currently on designing a compact Helium Synchrotron optimized for acceleration of proton and helium beams. Conventional Radiation Therapy makes use of X-rays that deliver most of their dose in healthy tissue before reaching the tumour. Protons and heavier ions, instead, present a characteristic Bragg peak, so they can be more precisely delivered to the tumour [1].

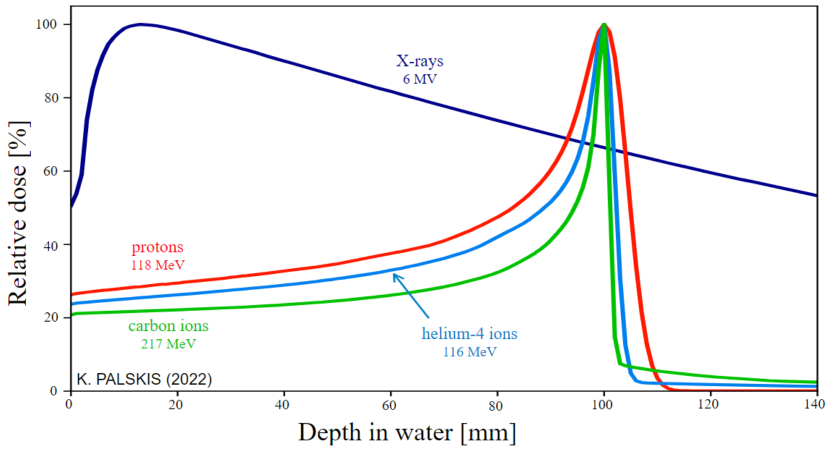

Figure 1: Energy deposition of X-rays, protons, carbon ions [2].

In recent years, there's been an increased interest in helium ions for cancer therapy because of a series of properties, including a sharper Bragg peak and the fact that it requires a smaller accelerator than a standard carbon ion synchrotron [3].
My project was focused on tune measurements during slow extraction for the Helium Synchrotron.

2 Theory

The Betatron tune is defined as the frequency of the particles' transverse oscillation in the accelerator. In fact, the particles don't follow a straight trajectory (the reference orbit), they oscillate. The full betatron tune, Q, is the number of these oscillations in one turn and can be split into two components: the integer part, number of complete oscillations during one revolution, and the fractional tune, q, representing the fractional difference in the phase of the oscillation from one turn to the next.

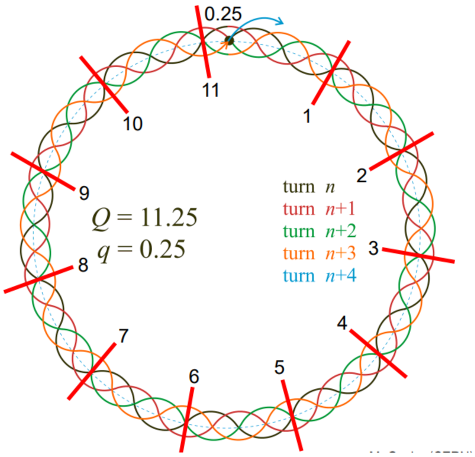

Figure 2: Representation of the tune of a beam in an accelerator [4].

When there is an imperfection at a given position along the ring, such that the particles receive a kick any time they pass, if the tune is an integer number, the amplitude of the oscillation increases at each turn up to the point where it is not stable anymore. In this condition, the integer resonance is excited. A similar effect also happens if the phase difference between two consecutive turns is 1/2 (second-order resonance), 1/3 (third-order resonance) and so on. This means that, in order to maintein the beam stable, these resonances should be avoided.
However, for slow extraction the particles are excited on purpose with the third-order resonance, so that their amplitude increases and they can be extracted continuously each turn.

The fractional part q can be determined using measurements from a specific monitor installed at one location in the machine. This monitor, a BPM (Beam position monitor), can measure the position of the beam with respect to the reference orbit. To do so, since the beam oscillation is often small, it is necessary to kick the beam so that the amplitude of the oscillations is increased and can be measured. From the particle position data, measured at a BPM monitor, the tune can be derived with various methods, based on FFTs.
While in measurements one looks at the signal of the entire beam, in simulations it is possible to compute the tune of the single particles and follow their individual behaviour. I have started from tracking simulations with the code X-Suite[5] and defined a "virtual" monitor to record the position of all the particles, turn by turn. To compute the tune I have used the NAFF function (Numerical Analysis of Fundamental Frequencies)[6]:

```
pnf.naff(signal, turns=500, nterms=1, skipTurns=0, getFullSpectrum=False, window=1)

signal          :   particle position data
turns           :   range of turns in which to calculate the frequency
nterms          :   maximum number of harmonics to search for
skipTurns       :   turns to skip at the beginning
getFullSpectrum :   if True uses a normal FFT
                    if False rFFT (only positive frequencies)
window          :   order of the window
```

The NAFF function performs a FFT (Fast Fourier Transform) on the turn by turn particle position, finds the peaks and then estimates more precise values by interpolating with a parabola.
The DFT (Discrete Fourier Transform) implicitly assumes that the signal is periodic, i.e. that the time series of length N repeats itself infinitely in a cyclic manner. Any resulted discontinuity spreads power all across the spectrum. The remedy is to multiply the signal with a window function before applying the DFT. This window function starts near or at zero, then increases to a maximum at the center of the time series and decreases again. Thus the discontinuity is removed and the calculation of the frequency is more accurate[7].
Therefore, using the NAFF method, the analyzed signal is first multiplied by a Hann window, that can be of different orders.

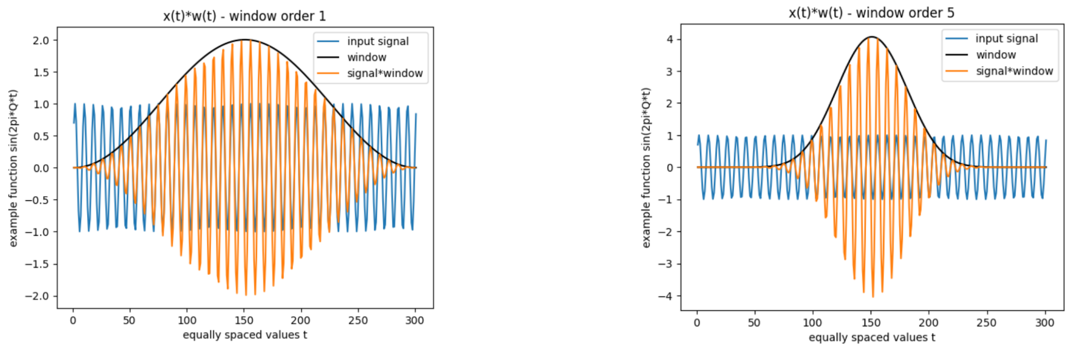

Figure 3: Windows used within the NAFF function and how they change the input signal.

The order changes the shape of the window: the higher the order the narrower the window will be.
Since we have no background noise in the simulations, the window order can be increased at will and this should result in increased accuracy in calculating the tune.
The aim of my project was to make the tune calculations as fast as possible. To do so, I defined in our simulations three monitors instead of one, so that every turn we get three positions.
The Nyquist-Shannon sampling theorem [8] states that the minimum number of samplings required to uniquely determine the frequency of a given signal is $2n_{cycles}$, i.e. $f_{sample} \geq 2f_{signal}$.
By implementing 3 monitors instead of one, we increase the sampling frequency, gaining precision in the tune calculation.
In particular, I put the first monitor over the sextupole and the other two symmetrically on the other two sides of the triangle:

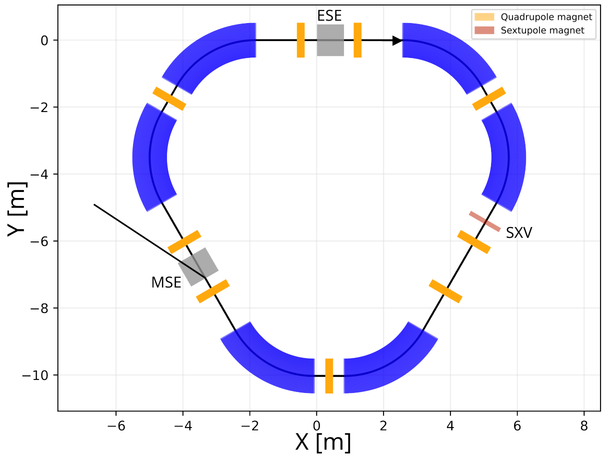

Figure 4: Representation of the Helium Synchrotron.

The first monitor was put on the sextupole because the Hamiltonian of the particles is calculated using the parameters from that position, so, in order to get the right orientation of the particles' trajectory in the Kobayashi-Hemiltonian plot (which will be shown later on) with respect to the contour lines, the particles position data had to be taken at the sextupole position.
Also, if the monitors are not equally spaced, this introduces an error, due to the change of the betatron oscillation along the ring.

Since the tune can change over time, for example during slow extraction, it is calculated through the use of "scrolling windows": the calculation is made over a range of turns that moves forward and both the length and the jump of this range can be set at will.

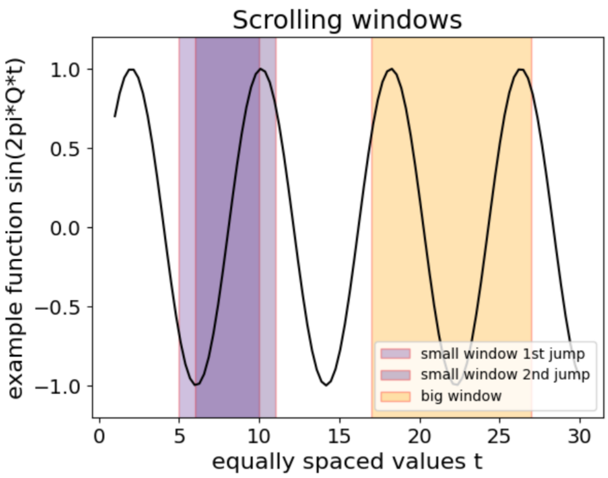

Figure 5: Examples of scrolling windows.

It is important that the window is short enough to approximate the tune as constant in that range, but long enough to observe a periodicity of the signal. The right length can be determined by the signal we are analysing, to capture its full behaviour.

I analyzed three cases:

- Stable Beam
- Betatron Core extraction
- RF-KO

In the first two I tracked the particles on xsuite using the parameters from the Helium Synchrotron, while in the third case I used pretracked particles [9] to compute their tune.

3 Stable Beam

The beam is located in the stable region near the third-order resonance excited by the sextuple (which is used to extract the beam).

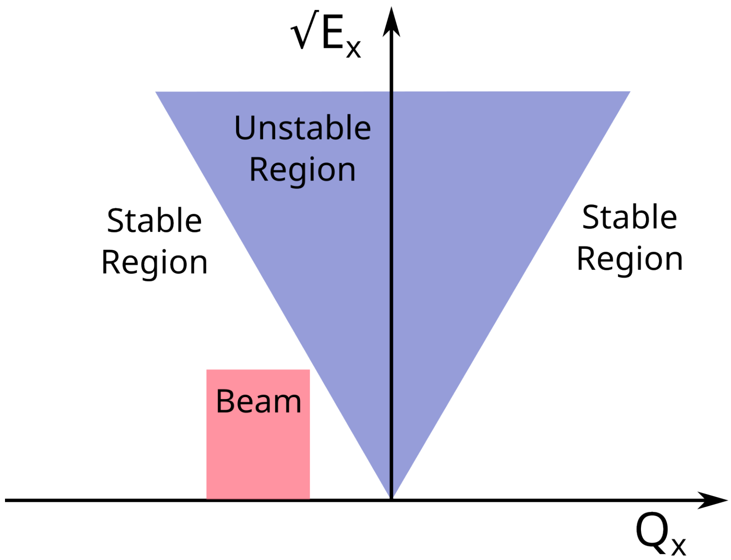

Figure 6: Steinbach Diagram for a stable beam near a third-order resonance excited by a strong sextupole[10].

I considered two subcases:

- Monoenergetic Beam
- Energy Spread

In the first case, the momentum spread of the particles is zero: $\frac{\delta p}{p} = 0$. This means that all the particles have the same energy and there is no spread around the reference energy.
In the second case $\frac{\delta p}{p} = 10^{-3}$, so there is a spread in energy.

3.1 Monoenergetic Beam

3.1.1 Tune calculations

In this case, the tune is constant over time.
The information we get from a virtual BPM is, for each particle, an array containing the position at each turn. By placing M BPMs and considering N turns, we obtain a matrix MxN for each particle, filled with the positions of the particles relative to the center of the beam. We can vectorize this matrix and obtain the following array:

$$x = x_1[1]x_2[1]...x_M[1]...x_1[N]x_2[N]...x_M[N] \tag{1}$$

This transformation results in the increase of the sampling rate from 1 sample/turn to M samples/turn. The new tune, using this method, is Q/M.
Using the NAFF method with just one monitor, the error on the tune Q (δQ) is $\frac{1}{N^4}$ (N is the number of turns), while with M monitors is $\frac{M}{(MN)^4}$. In our case M=3, so using 3 BPMs should be 27 times more accurate than using one.
To compute these tunes the arrays from the three monitors, with the positions of each particle, were merged as mentioned above, and the tunes were then calculated on the resulting arrays using the NAFF function with window of order 1.
The tune thus calculated is one-third of the actual tune, so the graphs with 3 monitors will always show the results multiplied by M=3.
From the following graphs we can see the difference in accuracy between the two methods (1 and 3 monitors).

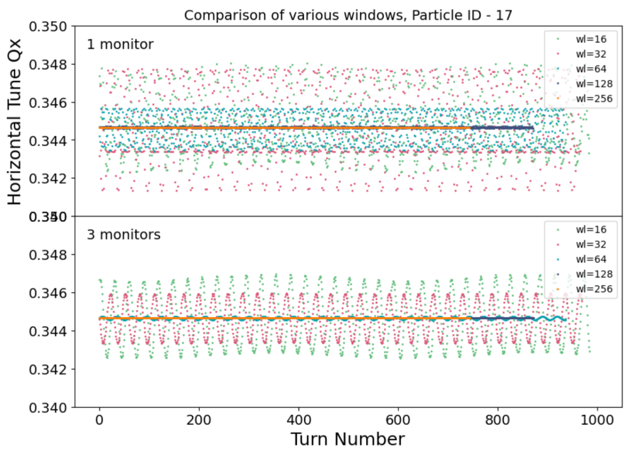

Figure 7: Comparison of five different windows, analysing the position data of a single particle from 1 and 3 monitors.

The greater the width of the window, the more the calculated tune will converge (as long as the tune is constant). In order for the NAFF function to work, the range in which the tune is calculated must be a multiple of 6, so any window that is not, is converted to the one of length 6*n closest to it (rounded down), as can be seen from the following graph. In fact, the calculated values are repeated in groups of 6.

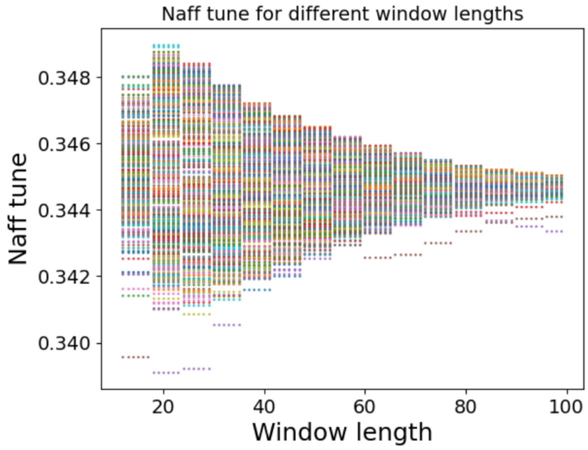

Figure 8: Plot of the tune calculated using different window sizes, in the range (12, 100), using 1 monitor. Each colour represents a different particle.

The data from window sizes in the range (6, 11) have been omitted because the error was not comparable with the others (almost three times bigger) and for values lower than 6 the naff function does not work.
All these tune values converge to the actual tune spread:

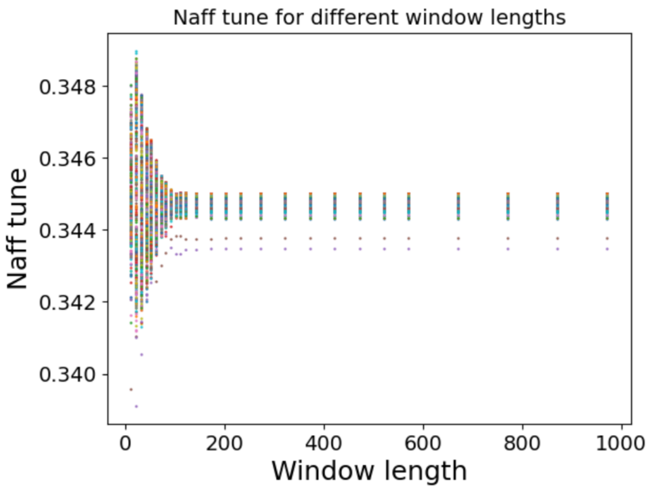

Figure 9: Plot of the tune versus window size used for the calculation, in range (12, 1000) (non-constant sampling), using 1 monitor.

A statistical analysis shows that the mean value to which the values calculated by naff converge is compatible with the nominal tune value defined in xsuite (calculated from twiss method).

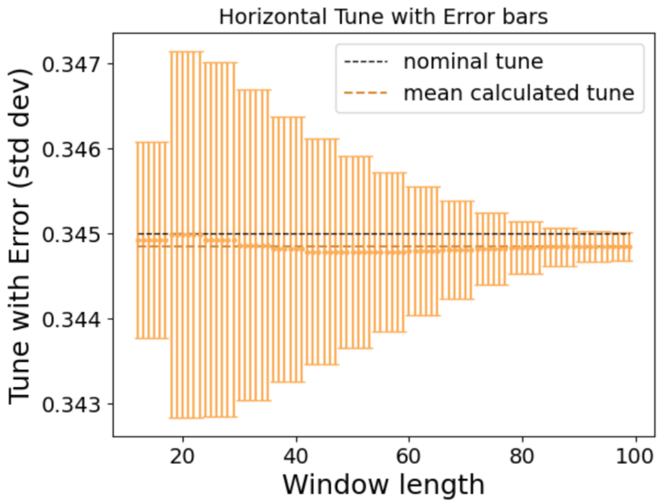

Figure 10: Statistical analysis of the calculated tunes.

Since the naff function converts the windows to multiples of 6, in the plot "Comparison of various windows", the actual windows were 12, 30, 60, 126 and 252.

As said before, increasing the window order should result in increased accuracy in calculating the tune, but it seems to make accuracy worse:

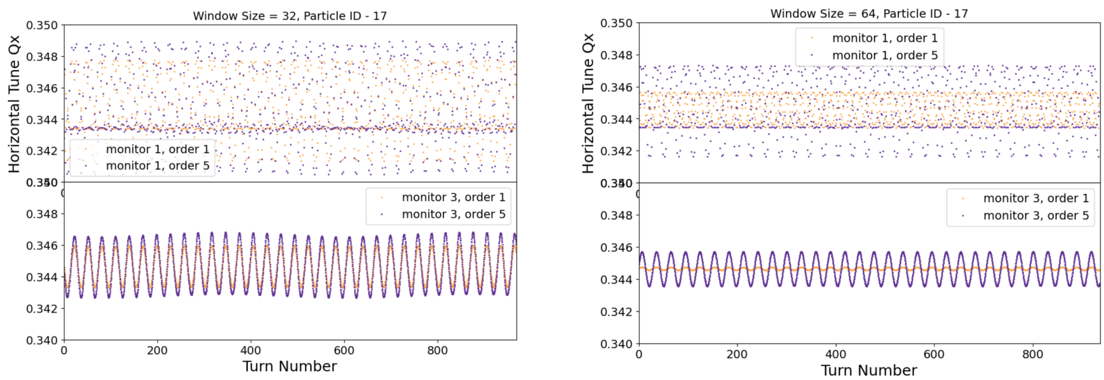

Figure 11: Comparison of tune calculations using an order 1 and order 5 window.

So from now on only order 1 will be used.

3.1.2 Hamiltonian

A useful tool that helps visualize the behaviour of the beam is the Hamiltonian: a mathematical description of the dynamics of the beam, depending on X and PX.

The Hamiltonian of particles near a third-order resonance excited by a strong sextupole is[11]:

$$H = \frac{\epsilon}{2}\left(X^2 + X'^2\right) + \frac{S}{4}\left(3XX'^2 - X^3\right) \tag{2}$$

where X and X' are the normalized coordinates:

$$X = \frac{x}{\sqrt{\beta_x}} \qquad X' = \frac{x\alpha_x}{\sqrt{\beta_x}} + x'\sqrt{\beta_x} \tag{3}$$

The following graph shows where the particles are located in the phase space: they are all inside the stable triangle. The lines represent different energetic levels (the Hamiltonians calculated as said before). Every particle is represented by a different colour.

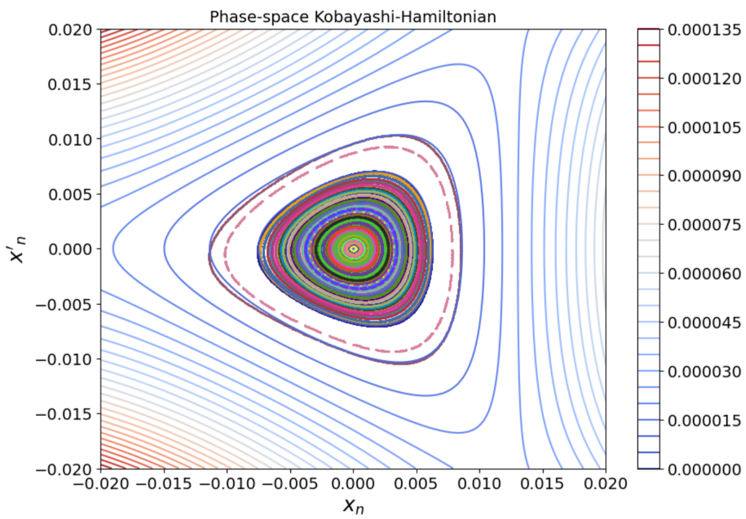

Figure 12: Kobayashi-Hamiltonian in normalized phase space with particles' trajectories (Poincaré section).

The Hamiltonian is approximately constant with time:

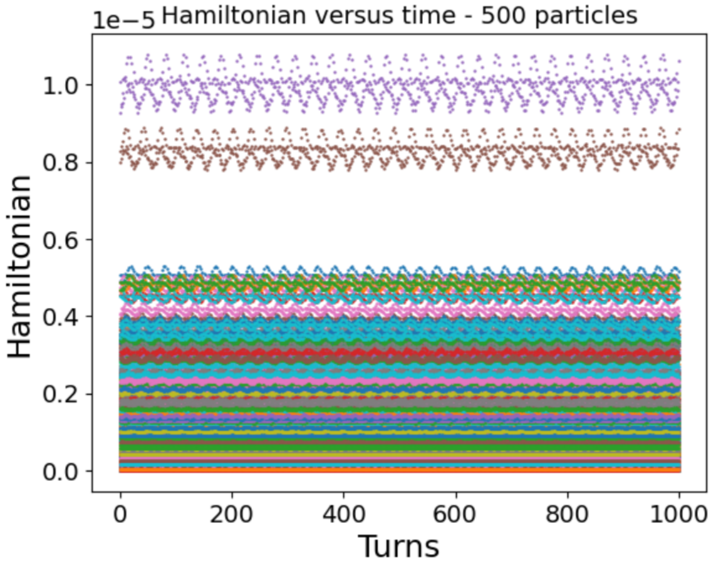

Figure 13: Hamiltonian of all the particles in the Beam as function of time. Each colour represents a different particle.

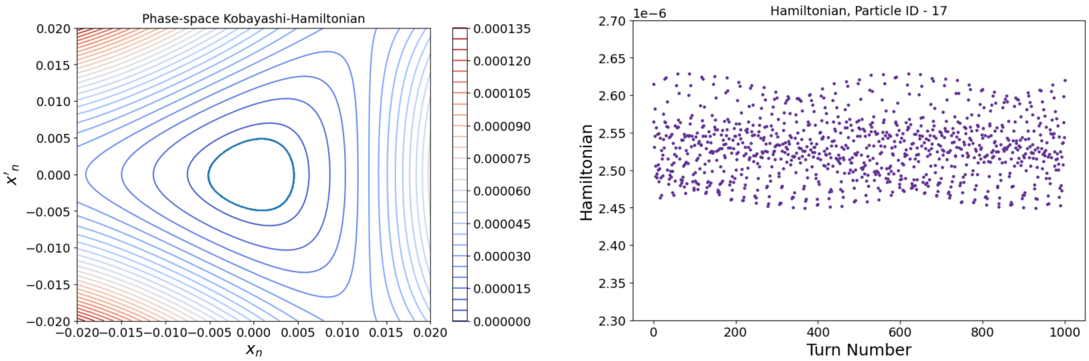

Figure 14: Kobayashi-Hamiltonian in normalized phase space and Hamiltonian versus time for a single particle.

3.1.3 Steinbach diagram

On the x-axis of the Steinbach Diagram we put the particles' tune, and on the y-axis the "effective, normalized amplitude of the betatron motion":

$$A_x = \sqrt{E_x/\pi} \tag{4}$$

where E_x is the ion's motion invariant sometimes referred to as the single-particle emittance.
If the position and momentum distributions of particles in the beam are known, then the Root Mean Square (RMS) emittance ϵ_{RMS} gives a statistical information on the area occupied by the entire

beam. The RMS emittance is defined as [12]:

$$\epsilon_{RMS} = \sqrt{\langle x^2 \rangle \langle {p_x}^2 \rangle - \langle x * p_x \rangle^2} \tag{5}$$

Where:

$${\sigma_x}^2 = \langle x^2 \rangle = \frac{1}{N} \sum_{i=1}^{N} (x_i - \bar{x})^2 \tag{6}$$

$${\sigma_{p_x}}^2 = \langle {p_x}^2 \rangle = \frac{1}{N} \sum_{i=1}^{N} (p_{x\,i} - \bar{p_x})^2 \tag{7}$$

$$\sigma_x \sigma_{p_x} = \langle x * p_x \rangle = \frac{1}{N} \sum_{i=1}^{N} (x_i - \bar{x})(p_{x\,i} - \bar{p_x}) \tag{8}$$

The action J_x is another particle invariant of motion. It has been defined as the area enclosed by the particle orbit divided by 2π. The generalised definition is:

$$\langle J \rangle = \langle \frac{A}{2\pi} \rangle = \epsilon_{\langle J \rangle} \tag{9}$$

In the following graph, instead, the amplitude of a single particle is computed as

$$A = \sqrt{\langle X^2 + X'^2 \rangle} \tag{10}$$

where X and X' are normalized according to Equation 3. The average in Equation 10, as well as the single-particles' tune, is calculated over 100 turns for 50 particles.

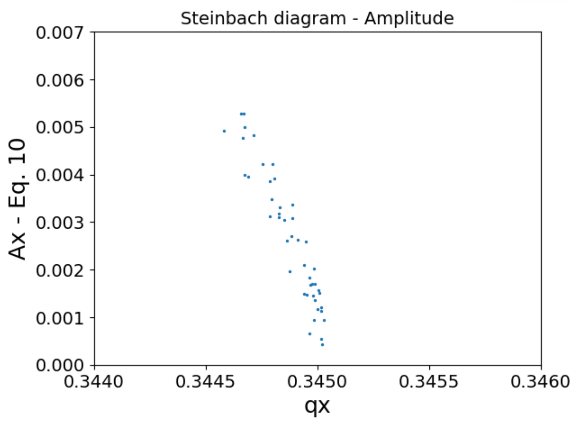

Figure 15: Steinbach diagram. Amplitude versus tune (Equation 10).

3.2 Energy Spread

In this case, in order to take into account the dispersion, it will be necessary to use a different set of coordinates, called betatron coordinates:

$$X_\beta = X - D_n \frac{\delta p}{p} \qquad {X_\beta}' = X' - {D_n}' \frac{\delta p}{p} \tag{11}$$

Note that when dispersion is zero ($\frac{\delta p}{p} = 0$) the two sets of coordinates are equivalent.

3.2.1 Tune calculations

The change of coordinates does not affect the calculation of the tune of an individual particle: each particle will have a different value of $D_n \frac{\delta p}{p}$, but, if this does not vary with time, the change of coordinates for the individual particle results in a simple rigid shift of positions, keeping the frequency (tune) unchanged.
This time, since $\frac{\delta p}{p} \neq 0$, the tune spread is bigger (it's proportional to chromaticity):

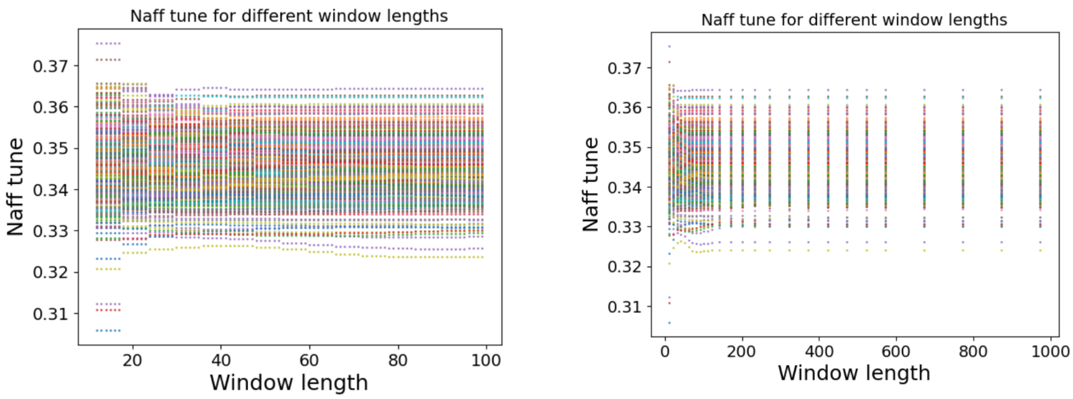

Figure 16: Plot of the tune calculated using different window sizes, using 1 monitor. Each colour represents a different particle.

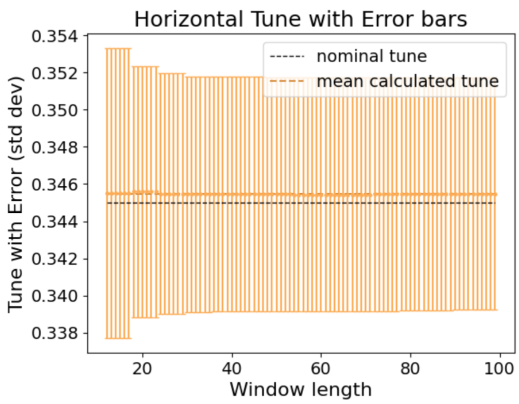

Figure 17: Statistical analysis of the calculated tunes.

3.2.2 Hamiltonian

If $\frac{\delta p}{p} \neq 0$, the Hamiltonian has to include a term that depends on the momentum deviation[11]:

$$H = \frac{1}{2}\left[\epsilon - 3S\left(D_n \frac{\delta p}{p}\right)\right]\left({X_\beta}^2 + {X_\beta}'^2\right) + \frac{S}{4}\left(3X_\beta {X_\beta}'^2 - {X_\beta}^3\right) \tag{12}$$

where X and X' are now replaced by the betatron coordinates.

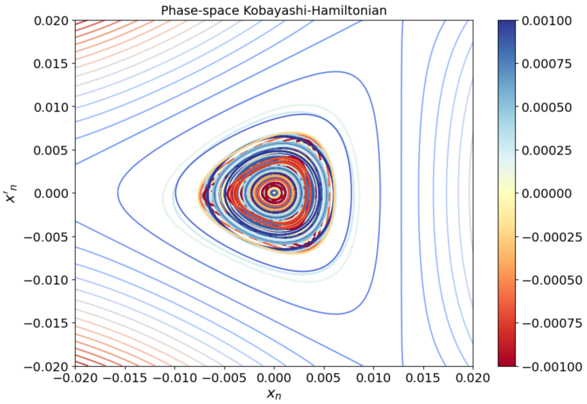

Figure 18: Kobayashi Hamiltonian in normalized phase space with particles' trajectories (Poincaré section).

The colours used for the particles trajectories represent the term of momentum deviation $\frac{\delta p}{p}$. The Hamiltonian lines are calculated putting this term to zero, so the particles with zero momentum deviation follow them perfectly, while the others have slightly different hamiltonians.
Note that in the previous case (zero momentum deviation) all the particles were following the hamiltonian lines.

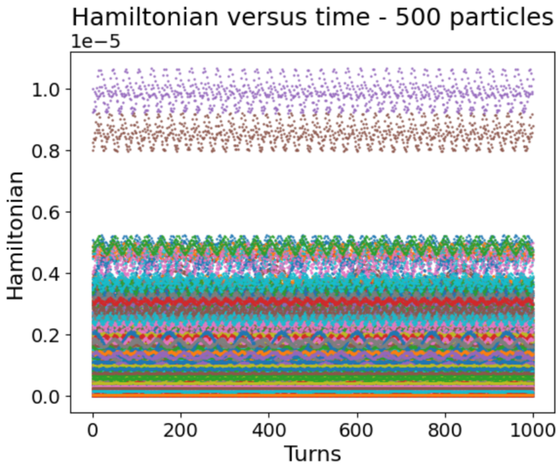

Figure 19: Hamiltonian of all the particles in the Beam as function of time. Each colour represents a different particle.

The following graphs show the trajectory of a single particle in the phase space and its hamiltonian over time.

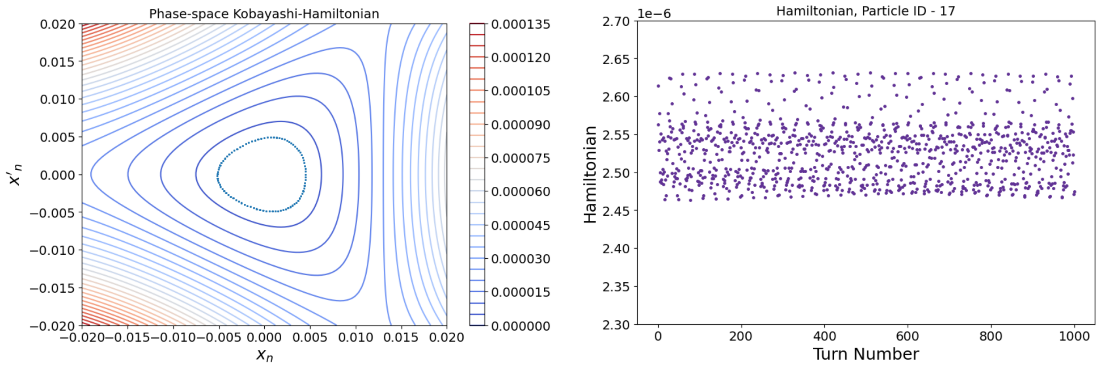

Figure 20: Kobayashi Hamiltonian in normalized phase space and Hamiltonian versus time of a single particle.

4 Betatron Core Extraction

The beam is pushed into the unstable region by a kick in momentum. This means that the tune is changing, approaching the third-order resonance.

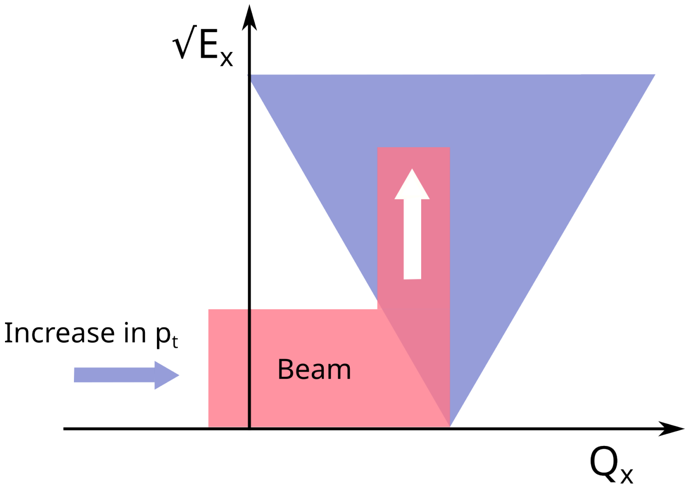

Figure 21: Steinbach Diagram for Betatron Core extraction [10].

The stable triangle shrinks with time, so that the particles gradually enter the unstable region and are extracted.

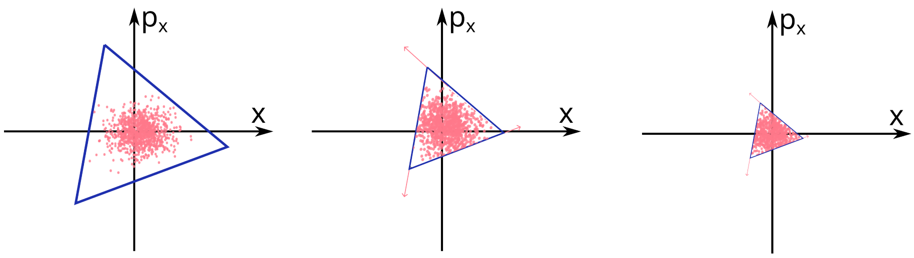

Figure 22: Representation of the Stable triangle evolution with Betatron Core extraction.

4.1 Tune calculations

With betatron core the tune changes linearly with time towards the third-order resonance.

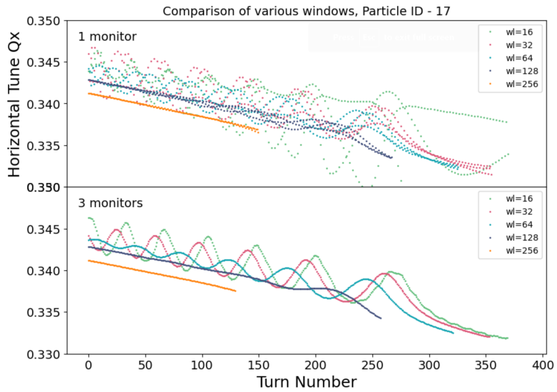

Figure 23: Comparison of five different windows, analysing the position data of a single particle from 1 and 3 monitors.

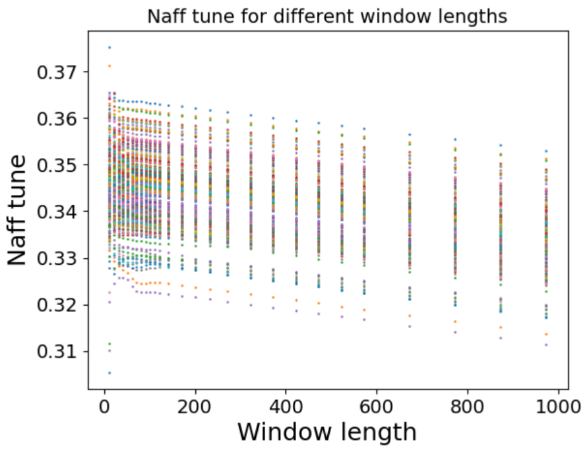

Figure 24: Plot of the tune calculated using different window sizes, in the range (12, 1000), using 1 monitor. Each colour represents a different particle.

4.2 Hamiltonian

The following graph shows the particles exiting the stable area.

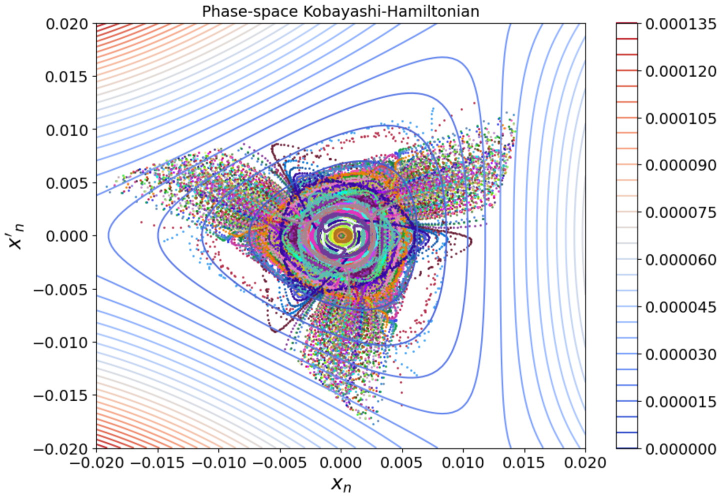

Figure 25: Kobayashi Hamiltonian in normalized phase space with particles' trajectories (Poincaré section).

In this case the contour lines are just a guide, because, as said before, during Betatron Core extraction the stable triangle shrinks with time, so these lines represent the stable triangle at turn zero.

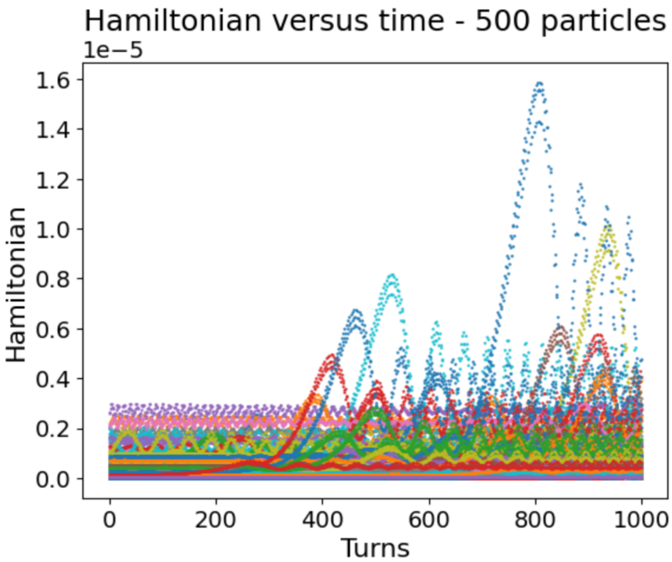

Figure 26: Hamiltonian of all the particles in the Beam as function of time. Each colour represents a different particle.

The Hamiltonian in not constant anymore over time: it increases as the particles are pushed outside the stable region.

For a single particle:

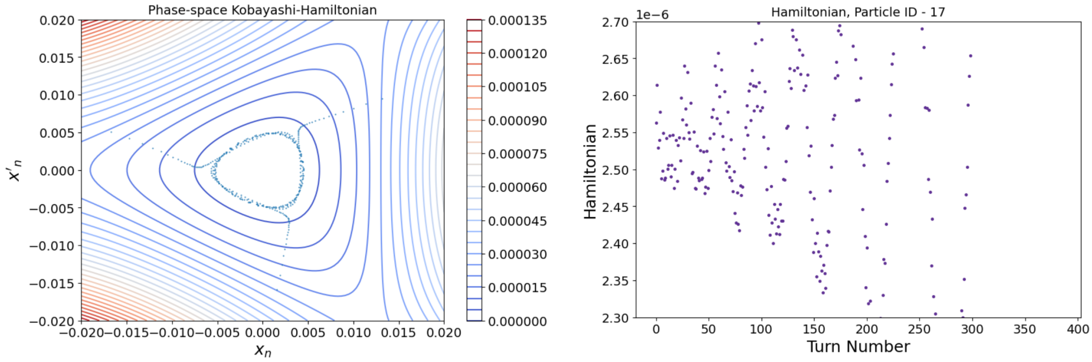

Figure 27: Kobayashi Hamiltonian in normalized phase space and Hamiltonian versus time of a single particle.

5 RF-KO

In this case the beam is pushed into the unstable region by a kick in amplitude, so that the tune doesn't change.

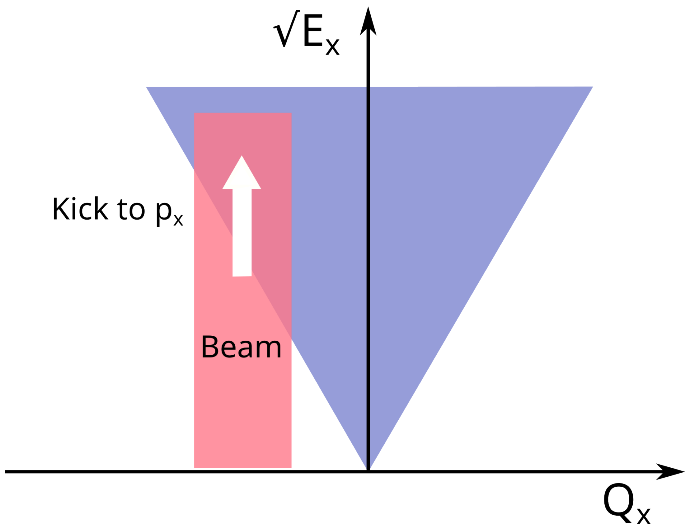

Figure 28: Steinbach diagram for RF-KO [10].

The stable triangle is now fixed, the particles are pushed outside by increasing their amplitude.

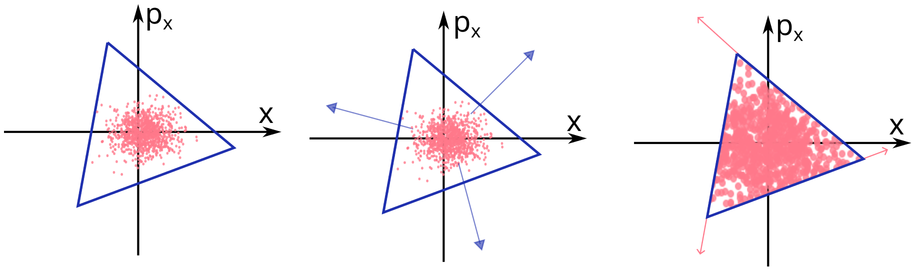

Figure 29: Representation of the Stable triangle evolution with RF-KO.

5.1 Tune calculations

This plot shows the comparison between different windows using 1 and 3 monitors.

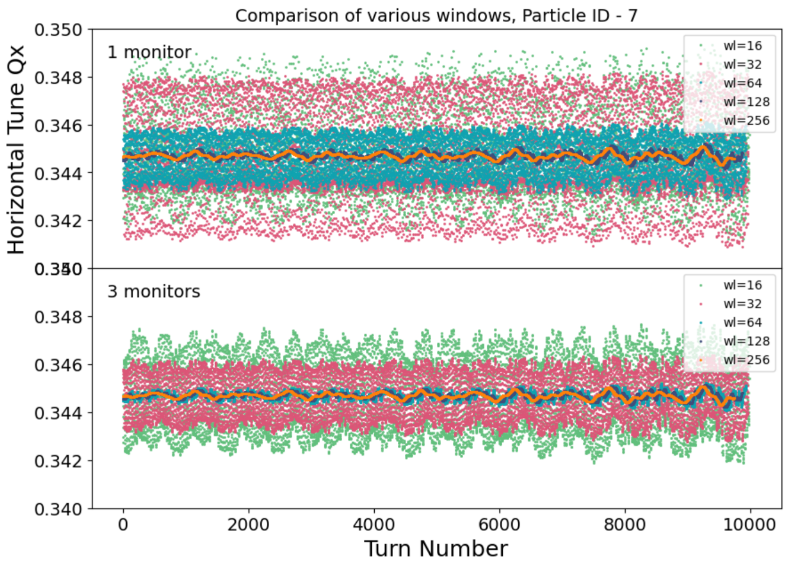

Figure 30: Comparison of five different windows, analysing the position data of a single particle from 1 and 3 monitors.

The tune is as predicted approximately constant.

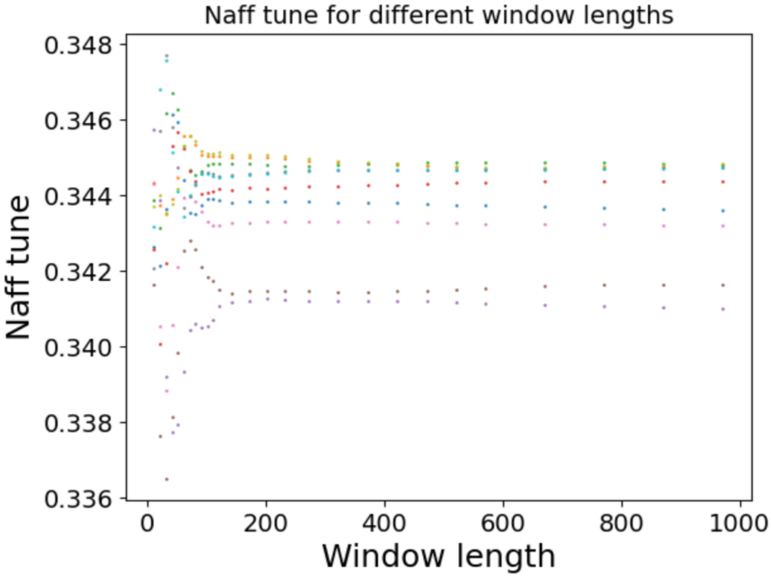

Figure 31: Plot of the tune calculated using different window sizes, in the range (12, 1000), using 1 monitor. Each colour represents a different particle.

Also in this case the tune values calculated using NAFF converge to the actual tune spread.

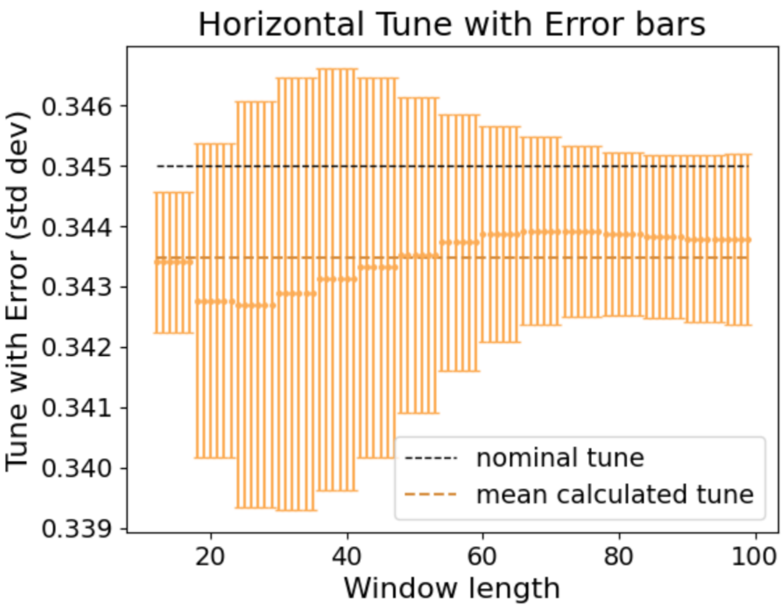

Figure 32: Statistical analysis of the calculated tunes.

5.2 Hamiltonian

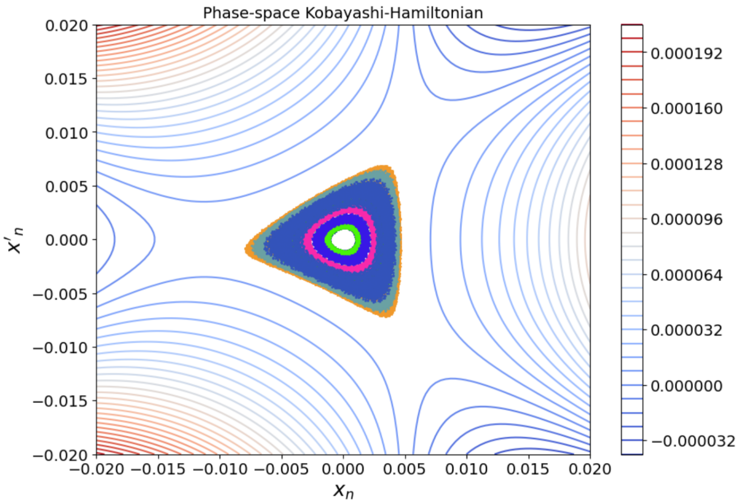

Figure 33: Kobayashi Hamiltonian in normalized phase space with particles' trajectories (Poincaré section).

The 10 particles of the beam are all in the stable triangle because they have not been extracted yet.

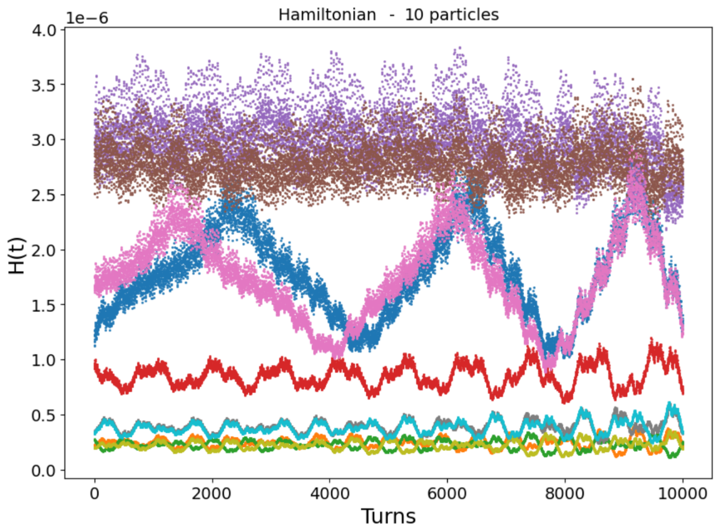

Figure 34: Hamiltonian of all 10 particles as function of time. Each colour represents a different particle.

6 Conclusions

The precision we want to obtain for the tune measurements is 10^{-2}, so, as shown in the following graphs, a window of length 16, using three monitors, is sufficient for this purpose in all three cases.

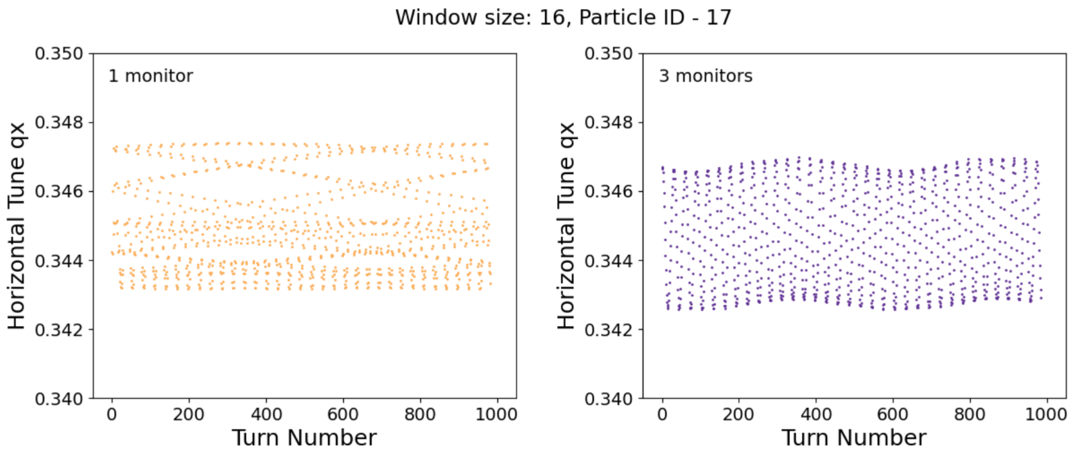

Figure 35: Tune calculated over 1000 turns with a window of 16 for a Stable Beam.

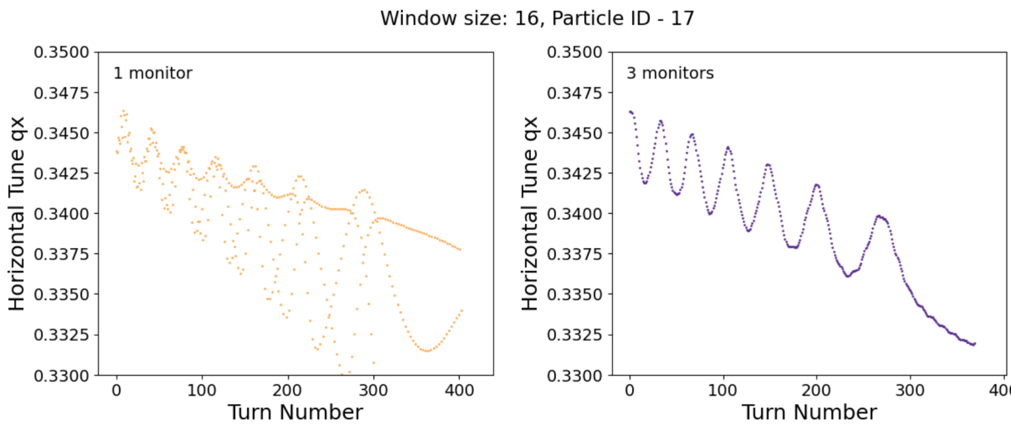

Figure 36: Tune calculated over 400 turns with a window of 16 for the Betatron Core extraction.

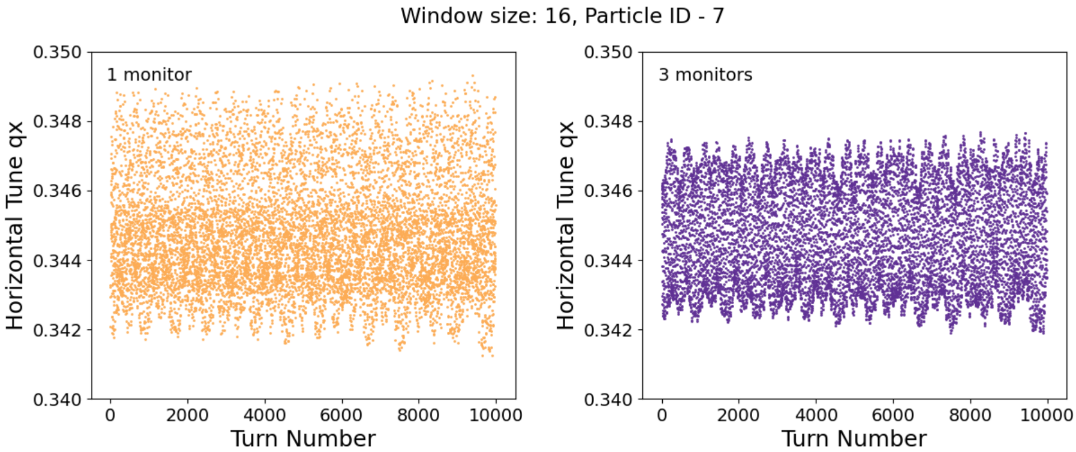

Figure 37: Tune calculated over 10000 turns with a window of 16 for RF-KO.

Since the naff function converts all the input window sizes to multiples of 6, the actual minimum number of turns in which the tune calculation is precise enough is 12.

References

[1] M. Vretenar. *A review of advanced particle therapy options.* URL: https://indico.cern.ch/event/1071872/contributions/4507688/attachments/2325124/3960391/NIMMS_baltics_10_21.pdf.

[2] M. Vretenar. *Conceptual design of a compact synchrotron-based facility for cancer therapy and biomedical research with helium and proton beams.* 2023. URL: https://indico.jacow.org/event/41/contributions/2845.

[3] M. Vretenar et al. *A compact Synchrotron for advanced cancer therapy with Helium and Protons Beams.* 2022. URL: https://cds.cern.ch/record/2813395/files/NIMMS_Note_010_Final.pdf?version=1.

[4] E. Wanvik. *Real-Time Schottky Measurements in the LHC.* 2018.

[5] R. Taylor. *private communication.*

[6] P. Zisopoulos F. Asvesta N. Karastathis. *PyNAFF.* URL: https://pypi.org/project/PyNAFF/.

[7] G. Sterbini P. Zisopoulos Y. Papaphilippou K. Skoufaris. *An update on the NAFF tool* $NAFF_U V$. 2019. URL: https://indico.cern.ch/event/797108/contributions/3312193/attachments/1801356/2938840/An_update_on_the_NAFF_tool.pdf.

[8] Wikipedia. *Nyquist–Shannon sampling theorem.* URL: https://en.wikipedia.org/wiki/Nyquist%E2%80%93Shannon_sampling_theorem.

[9] M. Detsi. *A Feedback controller for the RF-KO Method for Slow Extraction for NIMMS Helium Synchrotron.* 2023.

[10] Rebecca Taylor. *Extracting Fast and Slow. HITRI+ Heavy Ion Therapy MasterClass School.* 2021. URL: https://indico.cern.ch/event/1024183/.

[11] Accelerator Complex Study Group. *Proton Ion Medical Machine Study (PIMMS) PART I.* 1999.

[12] G. Russo. *Precise tune determination and split beam emittance reconstruction at the CERN PS synchrotron.* 2022.